Polymeric Carbon Dioxide

C.-S. Yoo

November 2, 1999

U.S. Department of Energy

Lawrence
Livermore
National
Laboratory

POLYMERIC CARBON DIOXIDE

CHOONG-SHIK YOO

Lawrence Livermore National Laboratory, Livermore, CA 94551, yoo1@llnl.gov

ABSTRACT

Synthesis of polymeric carbon dioxide has long been of interest to many chemists and materials scientists. Very recently we discovered the polymeric phase of carbon dioxide (called CO_2-V) at high pressures and temperatures. Our optical and x-ray results indicate that CO_2-V is optically non-linear, generating the second harmonic of Nd: YLF laser at 527 nm and is also likely superhard similar to cubic-boron nitride or diamond. CO_2-V is made of CO_4 tetrahedra, analogous to SiO_2 polymorphs, and is quenchable at ambient temperature at pressures above 1 GPa. In this paper, we describe the pressure-induced polymerization of carbon dioxide together with the stability, structure, and mechanical and optical properties of polymeric CO_2-V. We also present some implications of polymeric CO_2 for high-pressure chemistry and new materials synthesis.

INTRODUCTION

Application of high-pressure strongly perturbs the nature of chemical bonding, electronic and crystal structures, thermal, mechanical, and optical properties, and chemical reactivities of solids. These perturbations, which often occur systematically, provide opportunities for synthesizing new novel materials. Discoveries of a wide variety of materials unique to high P, T-conditions support this thesis; these include novel-gas compounds [4], metallic hydrogen [5], symmetric ice [6], superhard materials [7], high energy density polymers [8], and alkali-transition metal alloys [9]. Commonly used guidance suggestive to these discoveries has often been inferred from the electronic configuration, intermolecular interaction, crystal structure, effective close-packing and density, solubility and miscibility, group periodicity, and pressure-induced changes of these properties.

Molecular solids are described in terms of strong covalent bonds within molecules and weak van der Waals interactions between molecules. The strong intramolecular bonds make these molecules extremely stable at ambient conditions; whereas, the weak intermolecular interactions make such crystals very soft, at least initially at relatively low pressures. Because of this reason, many simple molecular solids particularly made of the first and second row elements such as CO_2, N_2, C, H_2O, CH_4, other C-N-O-H compounds are often considered as "inert" at relatively low pressures below 10 GPa. In fact, high stabilities of these molecules are often assumed even at very high pressures (10-40 GPa) and temperatures (1000-5000 K), as CO_2, N_2, H_2O, C are considered to be four major detonation products of energetic molecules.

At high pressures, however, the nature of these intermolecular interactions rapidly alters and becomes highly repulsive. Electron kinetic energy dominates, and electrons localized within intramolecular bonds become unstable. It is due to the higher power dependence of kinetic energy on density, $\rho^{2/3}$, than that of potential energy, $\rho^{1/3}$ (see Fig. 1). Therefore, at high pressures, the isolated electrons within intramolecular bonds are any longer stable, which leads to delocalization of the electrons through neighboring molecules. Such a modification of chemical bondings clearly results in soften of the stiff repulsive intermolecular potentials at high pressures and thus in physical and chemical phase transformations to a cross-linked two or three dimensional network structures. This perhaps is the reason for which the unsaturated molecular bonds become unstable above 10 GPa and which the network structures are ubiquitous at high pressures as can be seen in diamond, c-BN, β-C_3N_4, polymeric N_2, etc. [7,8].

Three mechanisms may occur at high pressures to delocalize electrons and soften repulsive potentials: (i) ionization creating attractive electrostatic energy, (ii) polymerization delocalizing intramolecular electrons between neighboring molecules, and (iii) metallization completely delocalizing electrons through conduction bands. These processes probably occur with increasing pressure as molecular phases → ionic species → polymeric phases → metallic phases. This conjecture is supported by our recent discoveries of the molecular-to-extended ionic and polymeric CO_2 phase transitions, both of which occur prior to the metallization at high pressures and temperatures [1-3]. In this paper we will describe the pressure-induced polymerization of CO_2 together with its stability, structure, and mechanical and optical properties.
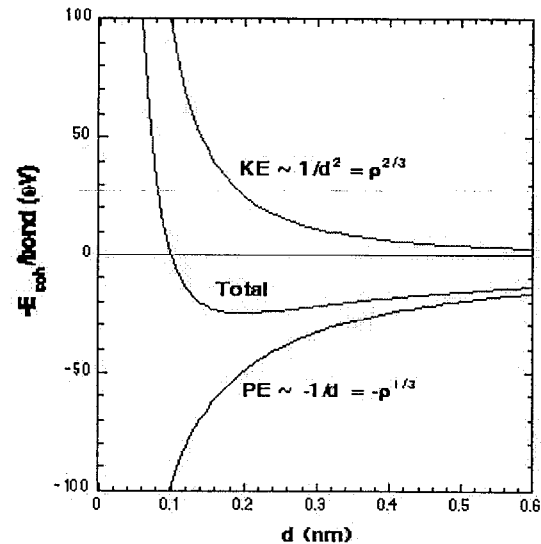

Fig. 1. The change of intermolecular interaction as a function of intermolecular distance (or density).

EXPERIMENT

The transformations of molecular solids to the extended phases often require relatively large positive volume changes (5-20 cm^3/mol) and, thus, are associated with large kinetic barriers (30-150 KJ/mol) [10]. As a result, these transitions are greatly hindered kinetically despite large thermodynamic stabilities of final products. Nitrogen may be a good example, in which system the polymerization has been suggested theoretically at about 60 GPa [8] but recent experiments indicate nitrogen being molecular even at 120 GPa [11].

In this study, we use a laser-heating technique to overcome the kinetic barrier existing in the molecular-to-extended phase transitions of carbon dioxide. Liquid CO_2 was loaded in a diamond-anvil cell (DAC) contained in a high-pressure vessel by condensing CO_2 gas at –40 ^{0}C and 10 atmospheres. The polymeric carbon dioxide was synthesized by heating carbon dioxide to high temperatures (>1800 K) at high pressures (>35 GPa) by using a Nd: YLF laser. However, because of the low absorption of carbon dioxide at the wavelength of Nd:YLF (1.054 μm), carbon dioxide was indirectly heated through ruby particles. Temperature of the sample was determined by fitting the thermal emission from the heated-area to a gray-body radiation formula.

The quenched products of CO_2 polymerization were investigated by using micro-Raman spectroscopy and synchrotron x-ray diffraction at both ESRF (ID-30) and SSRL (BL10-2). The determination of crystal structure of CO_2-V has been a challenge due to (I) the incomplete transformation resulting in a mixture phase of CO_2-III and V, (ii) relatively low-Z materials, (iii) complex, low symmetry crystal structure, (iv) highly strained lattice with strongly preferred orientation. Despite these difficulties, we were able to obtain reasonable diffraction patterns of various CO_2 phases including the polymeric phase by using highly intense x-ray beam at the 3rd generation synchrotron source. With a 10 μm-size focused monochromatic synchrotron x-ray beam and a fast scanning image-plate detector, we were able to obtain the angle-resolved x-ray diffraction selectively from a nearly completely transformed region of the sample.

The transitions and quenched products of CO2 were also characterized by micro-Raman spectroscopy using an Ar^+-ion laser, a triplemate, and a liq.-N_2 cooled CCD detector. The resolution of this system is within 1 cm^{-1}.

2

RESULTS AND DISCUSSIONS

Molecular Phases of CO_2

Carbon dioxide crystallizes to the cubic Pa3 structure, CO_2-I at 1.5 GPa and ambient temperature [12]. It is optically isotropic as shown in Fig. 2(a). Above 11 GPa, CO_2-I transforms to the orthorhombic Cmca phase, CO_2-III [12], which exists in a wide range of pressures above 70 GPa [3]. The large quadruple moment of linear CO_2 molecule is considered to stabilize both CO_2-I and III at least at relatively low pressures [13]. However, above 30 GPa, CO_2-III develops a very characteristic texture indicative of a highly strained lattice as shown in Fig. 2(b). It also shows an abnormally large pressure gradient exceeding 20 % of the maximum pressure of the sample within 100 μm. These observations clearly indicate that CO_2-III has high material strength at these pressures, which is rather unusual for a molecular crystal. In fact, the bulk modulus of CO_2-III has also been found to be unusually high 87 GPa, similar to that of elemental silicon [3]. For comparison, the bulk moduli of molecular phases are typically less than 15 GPa. The bulk moduli of various CO_2 phases will be discussed in details in the later section below.

Polymeric Phase of CO_2

Above 35 GPa and 1800 K, highly strained CO_2-III transforms into a new phase CO_2-V that can be quenched at ambient temperature as shown in Fig. 2(c). It clearly shows that the texture in transformed area is characteristic from that in untransformed area.

The phase transition from CO_2-III to CO_2-V is also evident from the Raman spectra obtained before and after heating a sample at 40 GPa as shown in Fig. 3. The Raman spectrum of CO_2-III is consisted of a few weakly resolved phonons between 250 and 500 cm^{-1}, typical for a highly strained molecular phase [14]. In contrast, the Raman spectrum of CO_2-V is different from the vibration characteristics of any known molecular polymorph of CO_2, suggesting that it has a different structure. We assigned the
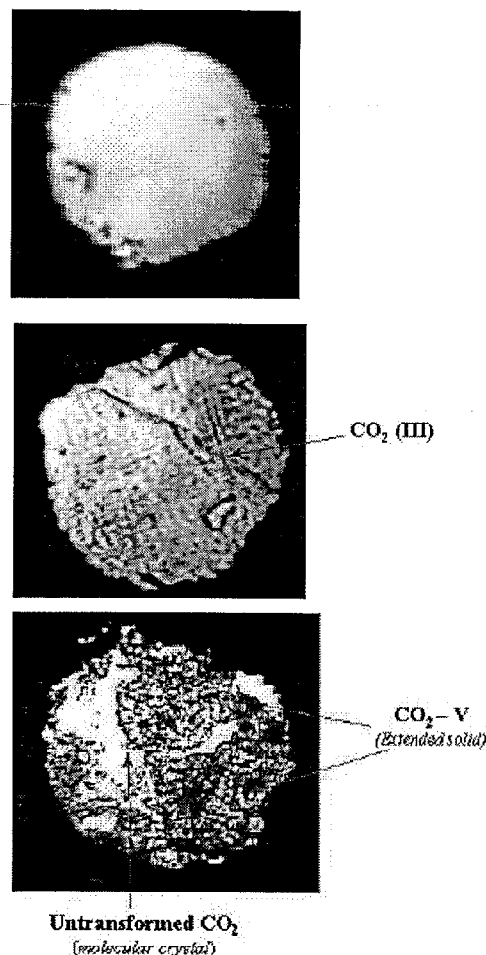

Fig. 2 Crystal phases of carbon dioxide: (a, top) CO_2-I, (b, middle) CO_2-III, (c, bottom) CO_2-V. CO_2-I and III are molecular phases; whereas, CO_2-V is an extended polymeric phase (see text).

most dominant vibration feature at 790 cm^{-1} to the symmetric stretch of the C-O-C bonds, v_σ(C-O-C). Based on the pressure dependence shown in Fig. 4, this mode should be located at 660 cm^{-1} at ambient conditions of pressure and temperature. This frequency of v_σ(C-O-C) is then translated into 398 - 491 cm^{-1} from the v_σ(Si-O-Si) mode in SiO_2 polymorphs, depending on the approximation used in the reduced-mass calculation [15]. This mass-weighted vibron frequency agrees reasonably well with v_σ (Si-

O-Si) frequencies in quartz at 464 cm^{-1} and in coesite at 510 cm^{-1} [15,16]. In contrast, the analogous mode of stishovite, a high-pressure polymorph of SiO$_2$, occurs at 750 cm^{-1} at ambient conditions [16], even a higher frequency than v_s (C-O-C) at 660 cm^{-1} of CO$_2$-V. The large pressure-dependent shift of

v_s(C-O-C) (Fig. 4) also is analogous to that of v_σ(Si-O-Si) in the coesite or quartz polymorphs of SiO$_2$. As previously explained for SiO$_2$ [16-18], the strong shift of v_σ(C-O-C) implies a high compressibility of CO$_2$-V as a result of a large change of C-O-C angles in this open structure.

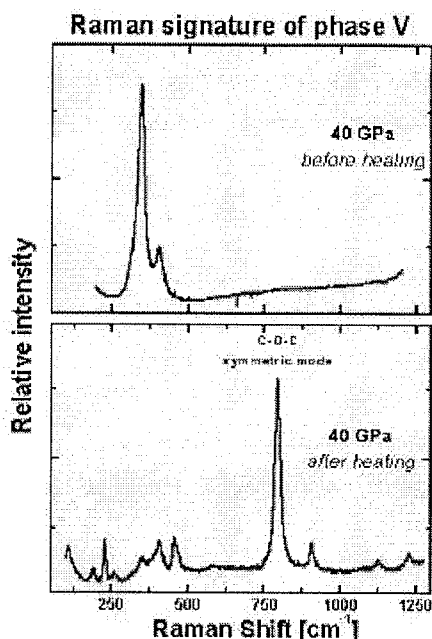

Fig. 3 Raman spectra of CO$_2$ obtained before and after the laser heating at 40 GPa, showing the phase transition from molecular CO$_2$-III to polymeric CO$_2$-V.
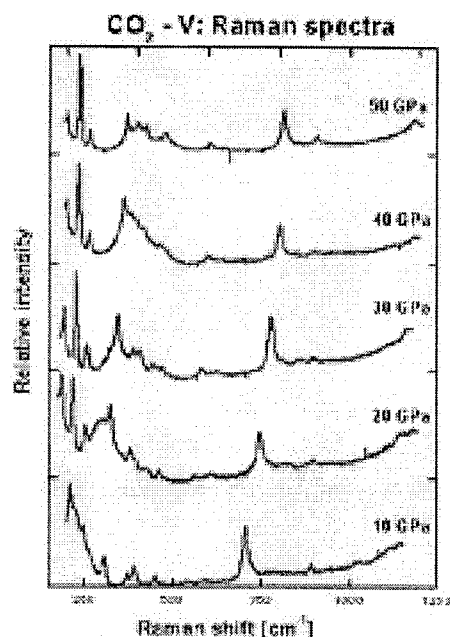
Fig. 4 Raman spectra of CO$_2$-V obtained during unloading at ambient temperatures. It shows that the CO$_2$-V can be metastably quenched at low pressures above 1 GPa.

Crystal Structure of CO$_2$-V

Figure 5 shows the diffraction pattern of CO$_2$-V at ambient temperature during unloading from 48 GPa. CO$_2$-V is clearly metastable at ambient temperatures over a large pressure range including the entire stability field of CO$_2$-III above 10 GPa. Below 10 GPa, CO$_2$-V begins to depolymerize to CO$_2$-I; however, diffraction peaks of CO$_2$-V remain even at 4 GPa. This observation is consistent with the earlier Raman data showing the C-O-C vibration band above 1 GPa.

The diffraction pattern of CO$_2$-V can be fit in terms of an orthorhombic structure with lattice parameters, a = 6.216 Å, b=4.352 Å, c = 6.066 Å at 48 GPa, consistent with 8 molecules per unit cell (Table I).

Fig. 5 Angle-resolved x-ray diffraction patterns of CO$_2$-V at several high pressures. The numbers indicate the pressures in GPa.

The intensity data and evidence for preferred orientation do not allow rigorous refinement of the structure. Nevertheless, we found a reasonable description of the diffraction pattern in terms of SiO_2-tridymite structures, particularly with an orthorhombic $P2_12_12_1$ structure that represents about 1/3 of a known SiO_2-tridymite unit cell [19,20]. The difference in the measured and calculated diffraction intensities was notable particularly for the 103 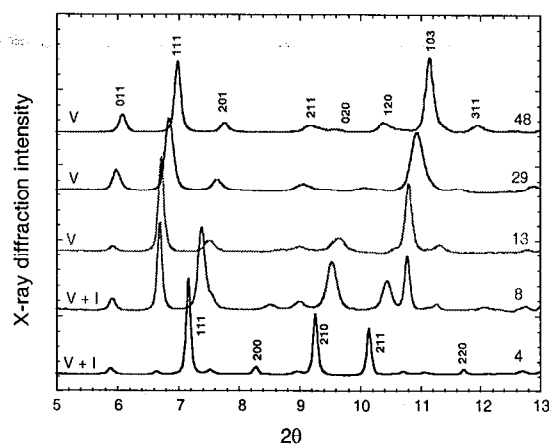reflection, probably due to the preferred orientation and/or disorder in the oxygen sublattice of the tridymite structure [21]. In fact, we have verified that introducing a slight disorder into the oxygen positions increases the intensity of the 103 reflection and makes it the strongest.

All tridymite structures can be derived from a parent hexagonal ($P6_3/mmc$) structure, a high temperature modification of β-SiO_2 quartz ($P6222_1$), by appropriate rotations of CO_4 tetrahedra [20,21]. In this "ideal" $P2_12_12_1$ tridymite structure of CO_2-V, each carbon atom is tetrahedrally bound to four oxygen atoms with the carbon-oxygen bond distances between 1.34(0.01) at 60 GPa and 1.40(0.01) Å at 10 GPa. The O-C-O angles are estimated to be 110(10)° (Fig. 6). These CO_4 tetrahedral units share their corner oxygens to form six-fold distorted holohedral rings with alternating tetrahedral apices pointing up and down the ab plane. The apices of tetrahedra are then connected through oxygen atoms along the c-axis. This interconnected layer structure of tetrahedra yields the C-O-C angle 130(10)°, substantially smaller than those of SiO_2-tridymites, 174°-180°.
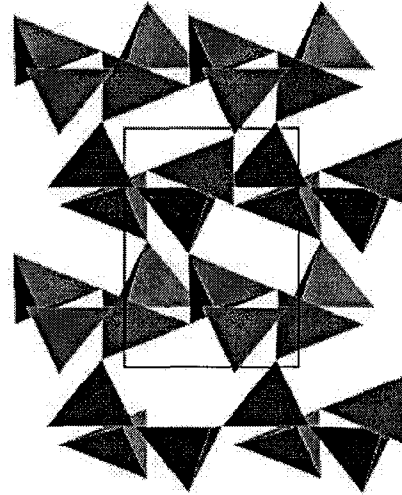

Fig. 6 An "ideal" crystal structure of CO_2-V in $P2_12_12_1$ with 8 molecules per unit cells. Carbon atoms are tetrahedrally bonded to four oxygen atoms, shown as CO_4 tetrahedra.

Table I. The crystal structure of CO_2-V ($P2_12_12_1$) at 48 GPa: a=6.216 Å, b=4.352 Å, c=6.066 Å, and ρ = 3.561 g/cm^3. The calculation was based on eight molecules per unit cell, and the final structure is analogous to that of SiO_2-tridymite (see the text).

hkl	d_{cal}(Å)	I_{cal}	d_{obs}(Å)	I_{obs}	Δd(Å)
011;110	3.536	20	3.531	27	0.005
111; 200; 002	3.074	100	3.066	96	0.008
201	2.766	13	2.766	17	0.000
211; 112	2.335	37	2.334	14	0.001
202; 020	2.171	14	2.161	3	0.010
120; 021	2.054	17	2.058	18	-0.004
103; 301; 310	1.923	33	1.923	100	0.001
311	1.788	20	1.793	14	-0.005
122; 203	1.701	12	1.700	2	0.001

Mechanical Properties

The EOS's of CO_2 phases have been determined as a function of pressures as shown in Fig. 7. CO_2-I transforms to CO_2-III at 12 GPa with no apparent volume discontinuity. The x-ray diffraction patterns between 10 and 20 GPa can be fit in terms of CO_2-I and III; no features are apparent for CO_2-IV. This may mean that the structure of CO_2-IV is similar to that of CO_2-III as suggested by the description, "distorted CO_2-III," used in earlier Raman studies [14]. The volume changes associated with this molecular-to-extended (III-to-V) transition vary between 15.3 % at 40 GPa and 12.6 % at 60 GPa, at ambient temperatures. Extrapolations of CO_2-V and III data yield the volumes 0.322 and 0.453 cm^3/g, respectively.

CO_2-I is soft, but both CO_2-III and V are very stiff solids as summarized in Table II. The bulk modulus B_0 of CO_2-I is 12.4 GPa typical for a molecular solid. In contrast, the B_0 of CO_2-III is unusually high 87 GPa, nearly in the range of Si (98 GPa) [22]. This result is consistent with the pressure gradient and observed texture in CO_2-III (Fig. 2(b)). Furthermore, the nearest neighbor C-O distance collapses to 2.303 Å at 40 GPa, from 3.135 Å at 1.5 GPa. These imply that CO_2-III is not entirely molecular; that is, the intermolecular bonding between neighboring CO_2 molecules is substantial. Such increased intermolecular bonding in CO_2-III at high pressures will certainly increase the strength of this material and act as a precursor for the transition to an extended phase like CO_2-V. The B_0 of CO_2-V (365 GPa) is much higher than that of SiO_2-quartz (37 GPa) or even stishovite (310 GPa) and is comparable to that of cubic-BN (369 GPa) [22]. This high bulk modulus and the large pressure gradient that CO_2-V supports lead us to conjecture that CO_2-V is a superhard polymer.
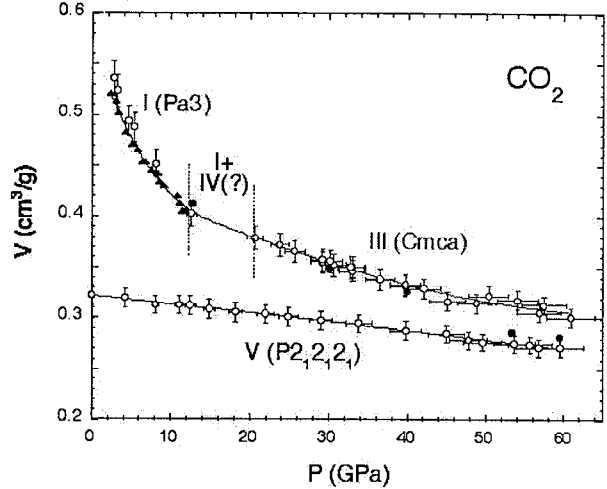

Fig. 7 Pressure-volume relations of CO_2 phases. The open circles with error bars are from this study; the solid triangles are from [23]. The calculated volumes of CO_2-III and V are also shown as the solid circles. The Birch-Murnaghan fits (lines) yield B_0=365 GPa for CO_2-V, 87 GPa for CO_2-III, and 12 GPa for CO_2-I.

Table II. The bulk moduli B_0 and their pressure derivatives B' of CO_2 phases in comparison with those of other covalently bonded solids [24,25].

Soilds	ρ (g/cm^3)	B_0 (GPa)	B'
Diamond	3.50	450	1.5
cubic-BN	3.48	369	4.0
CO_2-V	2.90	365	0.8
SiO_2-Stishovite	4.30	310	8.4
Al_2O_3-Corrundum	4.00	239	0.9
SiC	3.22	227	4.1
SiO_2-Coesite	2.92	96	8.4
SiO_2-Quartz	2.65	37	6.2
Silicon	2.33	98	4.2
CO_2-III	2.22	87	3.4
CO_2-I	1.75	12	4.5
δ-N_2	1.03	3	3.9

6

Optical Properties

CO_2-V is also an optically nonlinear solid, generating the second harmonic (SH) of Nd:YLF laser at 527 nm as shown in Fig. 8. The intensity of this sharp SH-band at 527 nm depends on how the Nd:YLF output is partitioned between heating and SH generation. The gray-body fit of the broad feature in Fig. 8 indicates that the temperature of the laser-heated area is 1670 K. We estimate the SH conversion efficiency of this new phase to be about 0.1%. The SH radiation was observed in all twenty samples that underwent the transition, indicating that the frequency doubling process is inherent to the new phase and does not rely on trace impurities that may be incorporated in the CO_2 lattice during heating. We also consider that the 0.1 % conversion efficiency is remarkably large based on the fact that the conversion efficiency is a nonlinear function of the incident laser power. In this study, we only used 10 W of a CW laser. Furthermore, the second harmonic was measured from a highly heterogeneous polycrystalline sample at 1670 K at 45 GPa, certainly not an ideal condition for the frequency conversion.

Symmetry considerations for SH generation processes provide further support that the crystal structure of CO_2-V is non-centrosymmetric like SiO_2 tridymite. Strong SH generation of light has been observed in solid forms of SiO_2, including crystalline, amorphous, and semiconductor-doped glass with a conversion efficiency up to 20 % [26,27]. The relatively sharp phonons and vibrons of CO_2-V (Fig. 3) imply that CO_2-V is not vitreous; SiO_2 glass is well known to have extremely broad vibration bands [16]. On the other hand, the SH process is symmetry forbidden in a crystal structure with a center of inversion [28]. This further excludes the possibility of CO_2-V being a centrosymmetric crystal like coesite or stishovite of SiO_2 [29,30]. Therefore, it is likely that the structure of CO_2-V is non-centrosymmetric like those of SiO_2-quartz, coesite, or tridymite, supporting the x-ray result.[19]
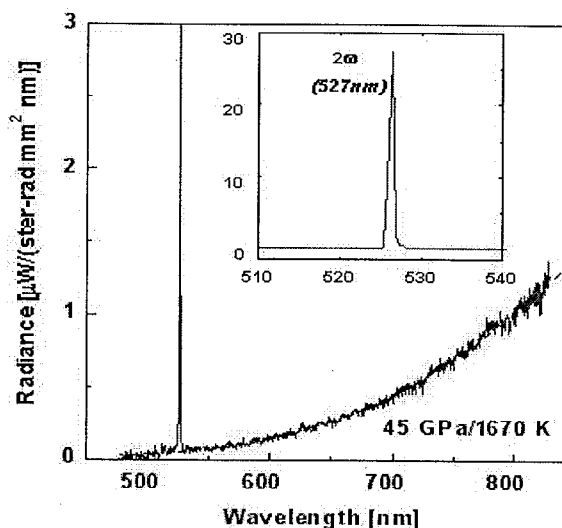

Fig. 8 The emission spectra obtained during Nd:YLF laser-heating of CO2-V, showing strong the second harmonic emission of the laser at 537 nm at 1670 K and 45 GPa.

CONCLUDING REMARKS

We discovered an optically non-linear, superhard polymeric CO_2-V at high pressures and temperatures. This is the first discovery of polymer made of CO_4 tetrahedra, for which synthesis has been of interest to many chemists and material scientists for many decades. This polymer crystallizes into an orthorhombic tridymite structure above 35 GPa and 1800 K and can be quenched at ambient temperature above 1 GPa. The tridymite structure of CO_2 is a high temperature modification of β-SiO_2 quartz, and there could be other high-pressure modifications of CO_2. Those include other four-fold coordinated CO_2 phases like cristobalites, quartz and coesites, three-fold carbonates, six-fold stishovite, and even amorphous CO_2 glass. The stability of such a wide-range of polymeric CO_2 phases if exist is likely strongly dependent on high pressures and temperatures, and the synthesis of such polymorphs in CO_2 is clearly a logical step for future studies.

This new extended polymeric phase of CO_2 has very important technological implications for developing high-power optical materials, high strength glass, and energetic materials, especially if it

7

can be recovered metastably at ambient pressure. This stems from high thermal conductivity and high energy density expected for this low-Z material. However, these new future material applications of CO_2 polymer should cope with several key synthetic new developments, which will be in many regards similar to how the first man-made diamond has been evolved to the large-volume synthesis, dynamic synthesis, and metastable CVD growth. Therefore, our current studies are focused on the recovery of CO_2-V at ambient condition and the development of alternative synthetic routes including metastable ones.

Carbon dioxide, together with nitrogen, carbon, and H_2O, has been considered to be one of the most stable molecules in a wide range of pressures and temperatures, as these molecules are considered to be four major detonation products of high explosives at 10-50 GPa and 2000-5000 K. The molecular-to-extended phase transition discovered in CO_2 is however contradict to the high stability of carbon dioxide and thus provides a new fundamental insight to the stability and structure of many other simple molecules at high pressures and temperatures. In fact, the extended forms of H_2, N_2, H_2O, NH_3, CO, C_2N_2, O_2 have already been experimentally observed and/or theoretically suggested. For example, N_2 has been suggested to transform into a polymeric black-P structure above 65 GPa [8]; C_2N_2 and CO polymerize below 12 GPa even at room temperature [31,32]. The symmetric H_2O and NH_3 recently discovered at high pressures are the extended phases [6,33]. The infrared-active H_2-III [34] and ε-O_2 [35] may indicate the initial charge separation between adjacent molecules (e.g. $H_2^{\delta+}H_2^{\delta-}$ and $O_2^{+}O_2^{-}$), precursors to the extended phases. Thus, it is important to *in-situ* investigate the structure and stability of simple molecules at high pressures and temperatures.

ACKNOWLEDGMENTS

REFERENCES

1. C.S. Yoo, H. Cynn, M. Nicol, *submitted* (1999).

2. V. Iota, C.S. Yoo, H. Cynn, *Science* **283**, 1510 (1999).

3. C.S. Yoo, et al., Phys. Rev. Lett. (1999) in print.

4. W.L. Vos. L.W. Finger, R.J. Hemley, J.Z. Hu, H.K. Mao, and J.A. Schouten, *Nature* **358**, 46 (1992).

5. S.T. Weir, A.C. Mitchell, W.J. Nellis, *Phys. Rev. Lett.* **76**, 1860 (1996).

6. A.F. Goncharov, V.V. Struzhkin, M.S. Somayazulu, R.J. Hemley, H.K. Mao, *Science* **273**, 218 (1996).

7. A.Y. Liu and M.L. Cohen, *Science* **245**, 842 (1989).

8. C. Mailhiot, L.H. Yang, A.K. McMahan, *Phys. Rev. B* **56**, 140 (1992).

9. L.J. Parker, T. Atou, J.V. Badding, *Science* **273**, 95 (1996).

10. R. van der Meer, A.L. German, and D. Heikens, *J. Poly. Sci.* **15**, 1765 (1977).

11. H. Lorenzana; *a private communication*

12. K. Aoki, H. Yamawaki, M. Sakashita, Y. Gotoh, and K. Takemura, *Science* **263**, 356 (1994).

13. R.D. Etters and K. Bogdan, *J. Chem. Phys.* **90**, 4537 (1989).

14. H. Olijnyk and A.P. Jephcoat, *Phys. Rev. B* **57**, 879 (1998).

15. The correspondence between the mode frequencies for the two structures can be estimated by considering the ration of the reduced vibrational masses for the symmetric stretching modes in singly bonded C-O-C and Si-O-Si structures. The angle between the two X-O single bonds is chosen to match the bond angle in α-quartz (104.6°). The low frequency limit (398 cm^{-1}) results from considering isolated structures (X_2O molecules) while the upper frequency (491 cm^{-1}) results by considering the second order shell of O atoms moving rigidly with the C (Si).

16. R.J. Hemley, in High Pressure Research in Mineral Physics, edited by M. H. Manghnani and Y. Syono, pp 347, (Terra Sci. Pub. Co., Tokyo, 1987).

17. S.K. Sharma, J.F. Mammone, M.F. Nicol, *Nature* **292**, 140 (1981).

18. J.D. Jorgensen, *J. Appl. Phys.* **49**, 5473 (1973).

19. A.K.A. Pryde and M.T. Dove, Phys. Chem. Minerals, **26**, 171 (1998).

20. R.F. de Dombal and M.A. Carpenter, Eur. J. Mineral **5**, 607 (1993) and references therein.

21. H. Graetsch and O.W. Flörke, Zeitschrift für Kristallographic **195**, 31 (1991).

22. E. Knittle, *"Mineral Physics and Crystallography, a Handbook of Physical Constants"* Edited by Ahrens, T., pp 98-142 (AGU, 1995); Knittle et al., Nature **337**, 349 (1989).

23. B. Olinger, J. Chem. Phys. **77**, 6255 (1982).

24. E. Knittle, *"Static Compression Measurements of Equation of State"* in *"Mineral Physics and Crystallography, a Handbook of Physical Constants"* Edited by Ahrens, T., pp 98-142 (AGU, 1995) and the references therein.

25. E. Knittle, R.M. Wentzcovitch, R. Jeanloz, M.L. Cohen, Nature 337, 349 (1989).

26. T.J. Driscoll and N.M. Lawandy, *J. Opt. Soc. Am.* **B11**, 355 (1994).

27. Y. Sasaki and Y. Ohmori, *Appl. Phys. Lett.* **39**, 466 (1981).

28. In general, the second harmonic of light is generated in non-centrosymmetric crystals; whereas, only odd harmonic are observed in centrosymmetric crystals. This stems from the second order polarization dependence of electromagnetic transitions. In crystals having a center of symmetry, the inversion of all coordinates must leave all relationships between physical quantities unchanged. Because the electric field **E** is odd under inversion operations, the polarization field **P** must also be odd, and the coefficients of all even powers in the

expansion of the polarization: $\mathbf{P} = \varepsilon_o \chi_1 \mathbf{E}\,sin\,(\omega t) + \varepsilon_o \chi_2 \mathbf{E}^2 sin^2\,(\omega t) + \varepsilon_o \chi_3 \mathbf{E}^3 sin^3(\omega t) + ...$ must vanish. In such crystals, only odd multiples of the incident frequency can be generated.

29. R.W.G. Wyckoff in Crystal Structures, vol 1, 2nd ed., pp 467 (Intersci., New York, 1963).

30. S.M. Stishov and V. Popova, *Geochem, Eng. Trans.* **10**, 923 (1961).

31. C.S. Yoo and M.F. Nicol, *J. Phys. Chem.* **90**, 6726 (1986); *ibid* **90**, 6732 (1986).

32. A.I. Katz, D. Schiferl, and R.L. Mills, *J. Phys. Chem.* **88**, 3176 (1981).

33. M. Gauthier, P. Pruzan, J.C. Chervin, and J.M. Besson, Phys. Rev. B **37**, 2102 (1988).

34. M. Hanfland, R.J. Hemley, H.K. Mao, Phys. Rev. Lett. 70, 3760 (1993).

35. Y. Akahama, H. Kawamura, S. Carlson, T. Le Bihan, and D. Hasermann, the abstract in a proceedings to the AIRAPT-17, Hawaii, July 25-30, 1999, p72; also L. Ulivi, R. Bini, F. Gorelli, M. Santoro, *ibid*, p73.